

Journal of Materials Chemistry A

Accepted Manuscript



This is an *Accepted Manuscript*, which has been through the Royal Society of Chemistry peer review process and has been accepted for publication.

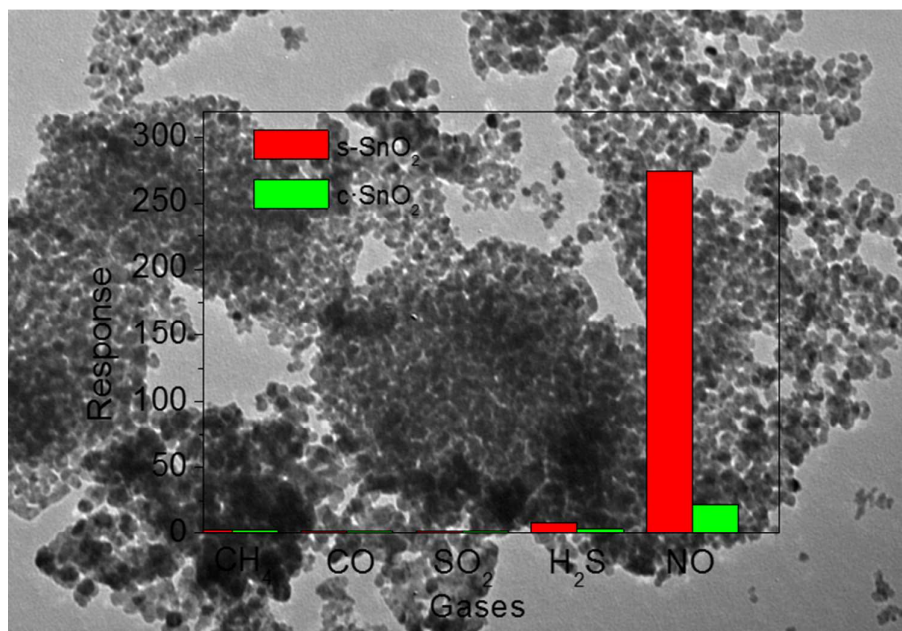
Accepted Manuscripts are published online shortly after acceptance, before technical editing, formatting and proof reading. Using this free service, authors can make their results available to the community, in citable form, before we publish the edited article. We will replace this *Accepted Manuscript* with the edited and formatted *Advance Article* as soon as it is available.

You can find more information about *Accepted Manuscripts* in the [Information for Authors](#).

Please note that technical editing may introduce minor changes to the text and/or graphics, which may alter content. The journal's standard [Terms & Conditions](#) and the [Ethical guidelines](#) still apply. In no event shall the Royal Society of Chemistry be held responsible for any errors or omissions in this *Accepted Manuscript* or any consequences arising from the use of any information it contains.

Porous SnO₂ Nanoplates for Highly Sensitive NO Detection

Fang Li, Yujiao Chen, Jianmin Ma*



Porous SnO₂ nanoplates with high NO response have been successfully prepared by the oxidization conversion of corresponding SnS₂ nanoplates.

Porous SnO₂ Nanoplates for Highly Sensitive NO Detection

Fang Li, Yujiao Chen, Jianmin Ma*

Received (in XXX, XXX) Xth XXXXXXXXX 200X, Accepted Xth XXXXXXXXX 200X

First published on the web Xth XXXXXXXXX 200X

DOI: 10.1039/b000000x

Porous SnO₂ nanoplates have been successfully prepared by the oxidation conversion of hydrothermally synthesized SnS₂ nanoplates at 500 °C. When exposed to NO gas, such porous SnO₂ nanoplate sensors have exhibited the fast response, enhanced sensitivity and excellent selectivity due to their unique structural characteristics in comparison with commercial SnO₂ nanoparticles.

Gas detection has been widely studied due to its importance in many fields.¹⁻⁴ As one of the most important gas detection devices, semiconductor gas sensors have drawn great attention, and great effort has been focused on the design and synthesis of sensing materials, since the gas-sensing performance of materials strongly depends on their size, shape, components and even impurities, which are determined by synthetic methods.⁵⁻¹⁵ Therefore, it is of interest to explore novel synthetic methods for improving the performance of sensing materials.

As an important n-type semiconductor, tin oxide (SnO₂) has obtained great attention in its application of gas sensors, since it has excellent gas-sensing characteristics.¹⁶⁻¹⁸ Presently, great effort has been focused on improving its gas-sensing properties, through controlling the size, shape, morphology of SnO₂,¹⁹⁻²³ as well as integrating other materials into SnO₂-based composites,²⁴⁻³⁰ respectively. Thus, it is necessary to prepare SnO₂ with novel synthetic methods for enhancing gas-sensing performance.

In this work, we have successfully developed an interesting synthetic route to prepare porous SnO₂ nanoplates by combining the hydrothermal synthesis and further oxidation of SnS₂ nanoplates. When porous SnO₂ nanoplates were used as the sensing material, the gas sensor displayed the excellent gas-sensing characteristics, such as the low work temperature as low as 200 °C, fast recovery time, and high sensitivity towards NO (494 for 20 ppm), and good selectivity to NO than other gases (CO, CH₄, H₂S and SO₂).

The porous SnO₂ nanoplates were synthesized by annealing hydrothermally obtained SnS₂ nanoplates using our previous synthetic method with slight modification.³¹ The phase and purity of the as-obtained SnO₂ nanoplates can be confirmed by the X-ray diffraction (XRD) and energy dispersive X-ray (EDX). The XRD patterns of SnO₂ nanoplates (Fig. 1) could be well indexed with the standard card (PDF: 41-1445). There is no impurities observed in the XRD patterns, which indicates that SnS₂ nanoplates can completely transferred into SnO₂ *via* the annealing and washing processes. The EDX spectrum of as-obtained SnO₂ was investigated (Fig. S1), which indicates there is no residue sulfur.

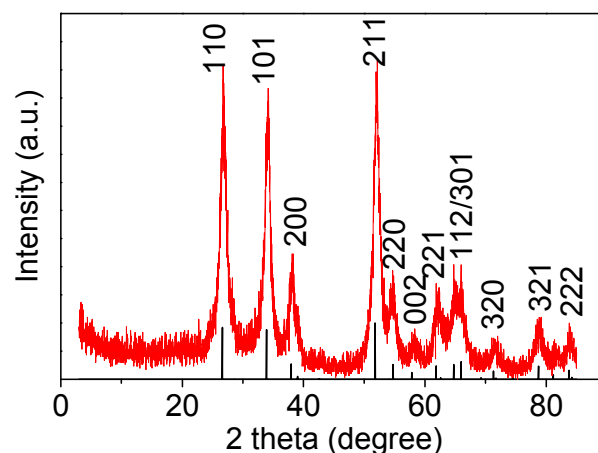


Fig. 1 XRD pattern of the as-obtained porous SnO₂ nanoplates.

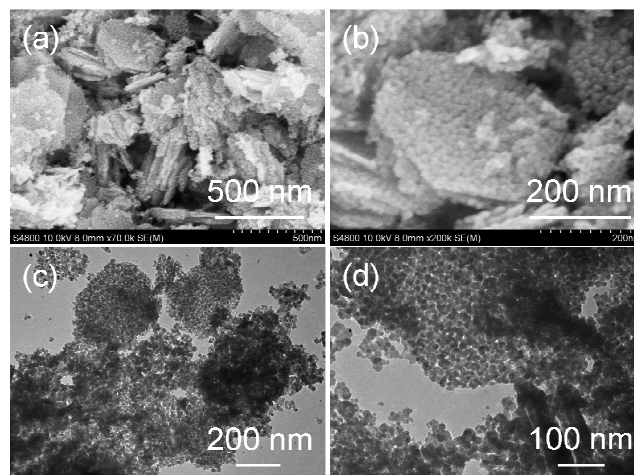


Fig. 2 (a and b) SEM images and (c and d) TEM images of the as-obtained porous SnO₂ nanoplates.

The morphology of SnO₂ nanoplates was characterized by the scanning electron microscopy (SEM) and transmission electron microscopy (TEM), respectively. Fig. 2a and b show the SEM images of SnO₂ sample. As shown in Fig. 2a, nanoplates can be observed, together with some particles. In the enlarged SEM image (Fig. 2b), one could find that the surface of SnO₂ nanoplate was not smooth. The structure of SnO₂ nanoplates were further analyzed by TEM. The TEM image (Fig. 2c) clearly indicates that SnO₂ sample is composed of nanoplates, together with some nanoparticles. In the enlarged TEM image (Fig. 2d), one could find that the nanoparticles on the surface of SnO₂ nanoplates have a size ranging from 5 to 8 nm. The above results indicate that it is

effective to synthesize SnO₂ nanoplates by annealing SnS₂ at 500 °C for 2 h. Other experimental results also proved this effectivity of such annealing technique.³²⁻³⁴

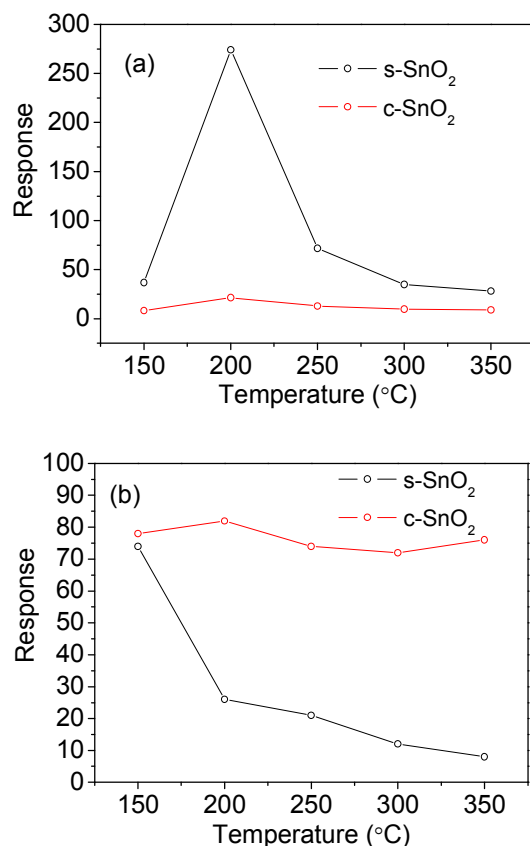


Fig. 3 (a) Sensitivity and (b) Response time of s-SnO₂ and c-SnO₂ sensors to 10 ppm NO gas at different working temperature.

Owing to their unique structure combining the plate-like shape and excellent porous characteristics, porous SnO₂ nanoplates are expected to demonstrate superior gas-sensing properties. Here, NO gas was chosen as the tested gas due to its high toxicity. Fig. 3a shows the response of the as-synthesized SnO₂ (s-SnO₂) and commercial SnO₂ (c-SnO₂) with a diameter of about 40 nm in Fig. S2) sensors towards 10 ppm of NO gas as a function of the operating temperature. For NO gas detection, the optimum working temperature should be about 200 °C, at which two sensors achieve the highest response towards NO gas from 150 to 350 °C. For s-SnO₂ and c-SnO₂ sensors in Fig. 3a, their highest response towards 10 ppm NO gas could reach 274 and 21.5, respectively. Moreover, the recovery time of both s-SnO₂ and c-SnO₂ sensors was studied, as shown in Fig. 3b. In Fig. 3b, one could find that the recovery time for the s-SnO₂ sensor can drop quickly from 74 s at 150 °C to 8 s at 350 °C. However, the recovery time for the c-SnO₂ sensor is always as long as above 70 s.

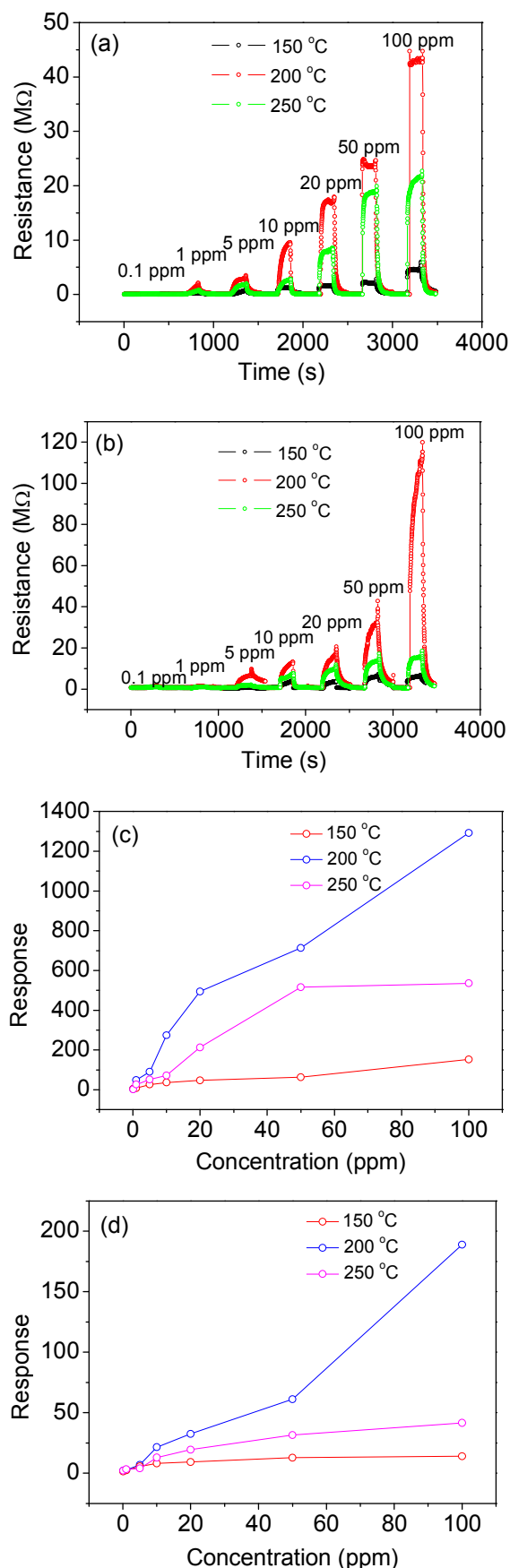


Fig. 4 (a and b) The real-time response curves of s-SnO₂ and c-SnO₂ sensors to NO gas with increased concentration at a working temperature of 200 °C, respectively; (c and d) The relationship between the sensitivity and NO gas concentration for s-SnO₂ and c-SnO₂ sensors, respectively.

To understand the NO gas sensing characteristics, the dynamic responses of both s-SnO₂ and c-SnO₂ sensors were investigated at three different temperatures (150 °C, 200 °C and 250 °C), respectively. The dynamic responses of both s-SnO₂ and c-SnO₂ sensors at 150 °C, 200 °C and 250 °C with various concentrations (0.1, 1, 5, 10, 20, 50 and 100 ppm) of NO gas are displayed in Fig. 4a and b, respectively. In Fig. 4a and b, one could find that the response amplitudes of both s-SnO₂ and c-SnO₂ sensors were increased with increasing the concentration of NO gas, respectively. In Fig. 4c and d, the corresponding response of both s-SnO₂ and c-SnO₂ sensors towards NO gas were found to be highest at 200 °C and enhanced with increasing the concentration of NO gas. Compared with the c-SnO₂ sensor (Fig. 4d), the response of s-SnO₂ sensor (Fig. 4c) is obviously higher. In Fig. 4c, the corresponding response of the s-SnO₂ sensor at 200 °C are 3.3 for 0.1 ppm, 49 for 1 ppm, 90.6 for 5 ppm, 274 for 10 ppm, 494 for 20 ppm, 713 for 50 ppm and 1292 for 100 ppm, respectively. The enhanced performance of porous SnO₂ nanoplates might be attributed to their unique plate-like structure and porous characteristics, which facilitate the process of NO oxidizing surface oxygen species of as-used SnO₂ material.³⁵ It is well known that SnO₂ is a n-type semiconductor. When SnO₂ sensor expose to oxidizing gas (NO, NO₂), the oxidizing gas will capture the free electron in SnO₂, resulting higher resistance.^{36, 37} Higher BET specific area of pore SnO₂ nanoplates may be also an important factor governing their better NO gas sensing performance. As shown in Fig. S3, the BET specific area of both s-SnO₂ and c-SnO₂ materials is 60 and 5.9 m²/g, respectively. The pore-size distribution was also further examined by using the Barrett–Joyner–Halenda (BJH) method, as shown in Fig. S4. The average pore diameter of the s-SnO₂ is approximately 6.27 nm, which is close to that obtained from the TEM observations.

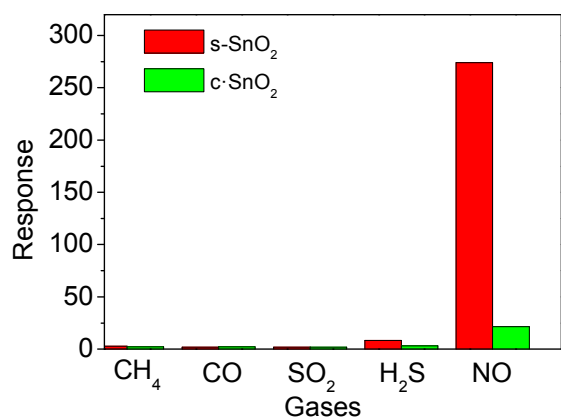


Fig. 5 Sensor response to various gases with 10 ppm at 200 °C.

The gas selectivity of both s-SnO₂ and c-SnO₂ sensors was also investigated in this work. Here, the response of both SnO₂ sensors towards other gases with 10 ppm was conducted, and the related results are shown in Fig. 5. In Fig.

5, one could find that two kind of SnO₂ sensors had a largely higher sensitivity towards NO than other gases, such as CH₄, CO, SO₂ and H₂S. In addition, we also studied the reproducibility of both s-SnO₂ and c-SnO₂ sensors. In Fig. 6a and b, the reproducibility of both s-SnO₂ and c-SnO₂ sensors demonstrates that the sensor maintains its initial response amplitude without a clear decrease upon ten successive sensing tests to 20 ppm NO gas. These results demonstrate that the s-SnO₂ sensor has better selectivity and stability than c-SnO₂ sensor towards NO gas.

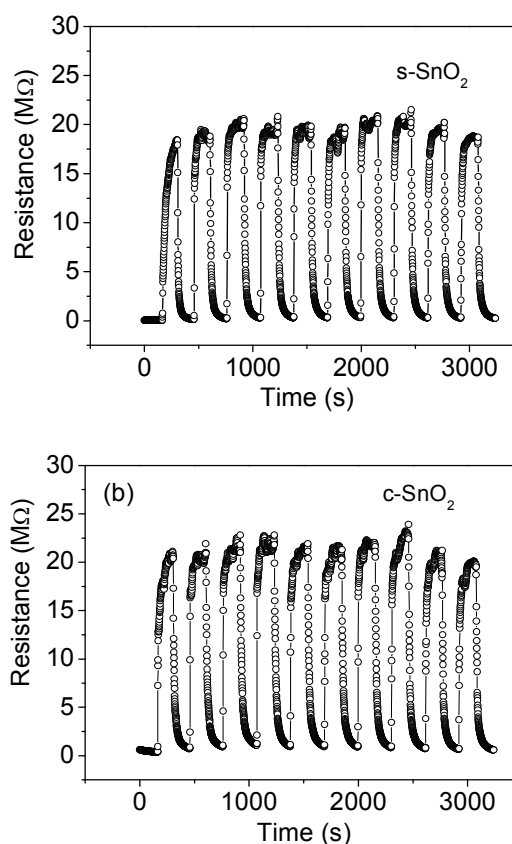


Fig. 6 (a and b) Reproducibility of s-SnO₂ and c-SnO₂ sensors on successive exposure (10 cycles) to 20 ppm NO gas.

In conclusion, we have successfully prepared the porous SnO₂ nanoplates by annealing the SnS₂ nanoplates obtained from the hydrothermal system. The structural characteristics and conversion of the as-synthesized SnO₂ nanoplates have also been studied. Gas-sensing results have demonstrated that the as-synthesized porous SnO₂ nanoplates had excellent gas-sensing characteristics towards NO gas with the lower working temperature, high selectivity, fast response and recovery, and high sensitivity. The as-synthesized porous SnO₂ nanoplates are expected to be a promising NO gas sensing material.

This work was supported by the National Natural Science Foundation of China (Grant No. 51302079).

Notes and references

Key Laboratory for Micro-Nano Optoelectronic Devices of Ministry of Education, State Key Laboratory for Chemo/Biosensing and

Chemometrics, Hunan University, Changsha, P. R. China. E-mail: nanoelechem@hnu.edu.cn (J. M. Ma),

† Electronic Supplementary Information (ESI) available: [details of any supplementary information available should be included here]. See DOI: 10.1039/b000000x/

‡ Footnotes should appear here. These might include comments relevant to but not central to the matter under discussion, limited experimental and spectral data, and crystallographic data.

- 1 J. E. Johnson, J. A. Shaw, R. Lawrence, P. W. Nugent, L. M. Dobeck and L. H. Spangler, *J. Appl. Remote Sens.*, **2012**, *6*, 063612.
- 2 J. Gu and C. L. Yang, *J. Petrol. Sci. Eng.*, **2010**, *73*, 233-237.
- 3 A. Safitri, X. D. Gao and M. S. Mannan, *J. Loss Prevent. Proc.*, **2011**, *24*, 138-145.
- 4 Y. J. Li and G. Wang, *Spectrosc. Spectr. Anal.*, **2011**, *31*, 3332-3335.
- 5 J. M. Ma, J. Teo, L. Mei, Z. Y. Zhong, Q. H. Li, T. H. Wang, X. C. Duan, J. B. Lian and W. J. Zheng, *J. Mater. Chem.*, **2012**, *22*, 11694-11700.
- 6 J. W. Deng, J. M. Ma, L. Mei, Y. J. Tang, Y. J. Chen, T. Lv, Z. Xu and T. H. Wang, *J. Mater. Chem. A*, **2013**, *1*, 12400-12403.
- 7 J. M. Ma, L. Mei, Y. J. Chen, Q. H. Li, T. H. Wang, Z. Xu, X. C. Duan and W. J. Zheng, *Nanoscale*, **2013**, *5*, 895-898.
- 8 M. Karimi, J. Saydi, M. Mahmoodi, J. Seidi, M. Ezzati, S. S. Anari and B. Ghasemian, *J. Phys. Chem. Solids*, **2013**, *74*, 1392-1398.
- 9 W. F. Qin, L. Xu, J. Song, R. Q. Xing and H. W. Song, *Sens. Actuators B: Chem.*, **2013**, *185*, 231-237.
- 10 W. Wen, J. M. Wu and Y. D. Wang, *Sens. Actuators B: Chem.*, **2013**, *184*, 78-84.
- 11 H. M. Zhang, C. Xu, P. K. Sheng, Y. J. Chen, L. Yu and Q. H. Li, *Sens. Actuators B: Chem.*, **2013**, *181*, 99-103.
- 12 S. Ashraf, C. S. Blackman, S. C. Naisbitt and I. P. Parkin, *Meas. Sci. Technol.*, **2008**, *19*, 025203.
- 13 J. M. Ma, J. Zhang, S. R. Wang, T. H. Wang, J. B. Lian, X. C. Duan and W. J. Zheng, *J. Phys. Chem. C*, **2011**, *115*, 18157-18163.
- 14 E. K. Heidari, E. Marzbanrad, C. Zamani and B. Raissi, *Nanoscale Res. Lett.*, **2010**, *5*, 370-373.
- 15 H. J. Xia, Y. Wang, F. H. Kong, S. R. Wang, B. L. Zhu, X. Z. Guo, J. Zhang, Y. M. Wang, S. H. Wu *Sens. Actuators B: Chem.*, **2008**, *134*, 133-139.
- 16 N. Barsan, M. Schweizer-Berberich and W. Göpel, *Fresen. J. Anal. Chem.*, **1999**, *365*, 287-304.
- 17 Y. J. Choi, I. S. Hwang, J. G. Park, K. J. Choi, J. H. Park and J. H. Lee, *Nanotechnology*, **2008**, *19*, 095508.
- 18 T. Kida, S. Fujiyama, K. Suematsu, M. Yuasa and K. Shimano, *J. Phys. Chem. C*, **2013**, *117*, 17574-17582.
- 19 D. F. Zhang, L. D. Sun, G. Xu and C. H. Yan, *Phys. Chem. Chem. Phys.*, **2006**, *8*, 4874-4880.
- 20 X. X. Xu, J. Zhuang and X. Wang, *J. Am. Chem. Soc.*, **2008**, *130*, 12527-12535.
- 21 Y. L. Wang, X. C. Jiang and Y. N. Xia, *J. Am. Chem. Soc.*, **2003**, *125*, 16176-16177.
- 22 B. Wang, L. F. Zhu, Y. H. Yang, N. S. Xu and G. W. Yang, *J. Phys. Chem. C*, **2008**, *112*, 6643-6647.
- 23 L. Y. Jiang, X. L. Wu, Y. G. Guo and L. J. Wan, *J. Phys. Chem. C*, **2009**, *113*, 14213-14219.
- 24 P. Li, H. Q. Fan and Y. Cai, *Sens. Actuators B: Chem.*, **2013**, *185*, 110-116.
- 25 A. Shanmugasundaram, P. Basak, L. Satyanarayana and S. V. Manorama, *Sens. Actuators B: Chem.*, **2013**, *185*, 265-273.
- 26 E. Nikan, A. A. Khodadadi and Y. Mortazavi, *Sens. Actuators B: Chem.*, **2013**, *184*, 196-204.
- 27 G. L. Cui, M. Z. Zhang and G. T. Zou, *Sci. Rep.*, **2013**, *3*, 1250.
- 28 G. J. Sun, S. W. Choi, A. Katoch, P. Wu and S. S. Kim, *J. Mater. Chem. C*, **2013**, *1*, 5454-5462.
- 29 L. L. Wang, J. N. Deng, T. Fei and T. Zhang, *Sens. Actuators B: Chem.*, **2012**, *164*, 90-95.
- 30 T. Yanagimoto, Y. T. Yu and K. Kaneko, *Sens. Actuators B: Chem.*, **2012**, *166*, 31-35.
- 31 J. M. Ma, D. N. Lei, L. Mei, X. C. Duan, Q. H. Li, T. H. Wang and W. J. Zheng, *CrystEngComm*, **2012**, *14*, 832-836.
- 32 P. K. Nair, M. T. S. Nair and J. Campos, *J. Electrochem. Soc.*, **1993**, *140*, 539-541.
- 33 D. N. Lei, M. Zhang, B. H. Qu, J. M. Ma, Q. H. Li, L. B. Chen, B. G. Lu and T. H. Wang, *Electrochim. Acta*, **2013**, *106*, 386-391.
- 34 Y. C. Zhang, Z. N. Du and M. Zhang, *Mater. Lett.*, **2011**, *19-20*, 2891-2894.
- 35 N. D. Hoa, N. V. Quy and D. Kim, *Sens. Actuators B: Chem.*, **2009**, *142*, 253-259.
- 36 I. Sayago, J. Gutiérrez, L. Arés, J. I. Robla, M. C. Horrillo, J. Getino, J. Rino and J. A. Agapito, *Sens. Actuators B: Chem.* **1995**, *26-27*, 19-23.
- 37 L. Wang, Y. J. Chen, J. M. Ma, L. B. Chen, Z. Xu and T. H. Wang, *Sci. Rep.*, **2013**, *3*, 3500.